Interplay of electrostatic and van der Waals forces in coronene dimer

4 AUTHORS, INCLUDING:

O. I. Obolensky
National Center for Biotechnology Informat…
40 PUBLICATIONS **239** CITATIONS

SEE PROFILE

Veronika V. Dick
Fraunhofer Institute for Industrial Mathem…
12 PUBLICATIONS **82** CITATIONS

SEE PROFILE

Interplay of Electrostatic and van der Waals Forces in Coronene Dimer

O. I. OBOLENSKY,[1] V. V. SEMENIKHINA,[2] A. V. SOLOV'YOV,[1] W. GREINER[1]

[1]*Frankfurt Institute for Advanced Studies, Johann Wolfgang Goethe University, Max von Laue str. 1, D-60438 Frankfurt am Main, Germany*

[2]*Frankfurt Graduate School of Physics, Johann Wolfgang Goethe University, Max von Laue str. 1, D-60438 Frankfurt am Main, Germany*

ABSTRACT: Interplay of electrostatic and van der Waals forces in the coronene dimer is studied. Our results show that the lowest-energy configuration of the dimer is not necessarily a stack, as it might had been expected a priori. This is a surprising result for the dimer of such a large polycyclic aromatic hydrocarbon (PAH) as coronene ($C_{24}H_{12}$). The energy of the T-shaped configuration at all highest feasible levels of density functional theory (DFT) (B3LYP, PBE/6-31+G(d), D95, cc-pVDZ, cc-pVTZ) is lower than the energies of the three plausible stack configurations. To get a better description of the van der Waals interaction, the DFT results were corrected by a phenomenological van der Waals-type term. This correction gives a slight edge to the parallel-displaced stack configuration. However, the magnitude of the correction is somewhat arbitrary, depending on the set of parameters used. This makes the definitive conclusion impossible at the currently achievable level of theory. A simple model is proposed that is useful for the qualitative understanding of possible geometries of the coronene dimer and larger coronene clusters. The model represents the coronene dimer as two sets of charged rings interacting via Coulomb and Lennard-Jones potentials. The model provides an intuitively clear explanation as to why the T-shaped dimers can be of importance even for some of moderately large PAHs such as coronene, and perhaps for circumcoronene as well. The unexpectedly strong competitiveness of the T-shaped

---

configuration is connected to the round shape of the coronene molecules. Indeed, rotation or parallel displacement of the non-round monomers result in significantly smaller Coulomb repulsion as compared with the "face-to-face" sandwich configurations. In contrast, for the stacked round molecules rotation and/or displacement are much less effective. Therefore, the round shape of the coronenes leads to an increased role of the electrostatic repulsion in the stack configurations. The proposed model can easily be generalized to other PAH, DNA bases, etc.   © 2006 Wiley Periodicals, Inc. Int J Quantum Chem 107: 1335–1343, 2007

1. Introduction

Molecules of polycyclic aromatic hydrocarbons (PAHs) and their ions are of current interest, as they are believed to be one of the most probable species in the interstellar space responsible for converting the ultraviolet (UV) radiation of stars into the intensive infrared (IR) radiation, known as unidentified IR bands [1–7]. The physical mechanisms and effectiveness of energy transfer from the UV to the IR radiation occurring via transient heating [8] are currently being studied (see, e.g., Refs. [1, 9–11]).

Astrophysical observations suggest that the interstellar medium contains a variety of small carbonaceous particles, with sizes ranging from dust grains down to single molecules [12]. The most abundant particles contain 100–1,000 carbon atoms [13] in the forms of collections (clusters) of PAH-like molecules [10] of various degrees of hydrogenation [2]. Hence, studying properties of PAH clusters presents a necessary step in further research of the interstellar medium.

The current knowledge of structure and ways of formation of PAH clusters is very limited. Laboratory studies have just begun to appear; only anthracene [14, 15], naphthalene [14], and coronene [16, 17] clusters have been produced so far, so that the array of available experimental data is sparse. Theoretical investigations of oligomers of the larger PAHs are also scarce; furthermore, their results are very sensitive to a subtle interplay between the van der Waals polarization forces (also sometimes called dispersive interaction) and the electrostatic interaction. Even for benzene, the simplest aromatic hydrocarbon, an unequivocal choice between the T-shaped and the parallel-displaced stack configurations, is a challenging problem, since the difference in binding energies for these configurations is comparable to accuracy of the calculations even at

the most advanced levels of theory [18–20]. Alternative approaches based on mixing of the ab initio and the phenomenological treatments have been suggested that permit a more flexible tuning of interactions (see, e.g., [21–25]), but their universality and predictive power remain unclear.

We have performed density functional theory (DFT) calculations of energies for four plausible configurations [22] of the coronene dimer. These include three stack configurations [i.e., superimposed stack "sandwich" (SS), twisted stack (TS), and parallel-displaced (PD) stack] and the T-shaped configuration. To our knowledge, this is the first comparative study of the configurations of the coronene dimer within the ab initio approach. The only other ab initio calculation of the coronene dimer parameters was done for the PD stack configuration [21].

The energy of the T-shaped configuration at all currently feasible levels of theory (combinations of the B3LYP and PBE functionals with 6-31+G(d), D95, cc-pVDZ, and cc-pVTZ basis sets) was systematically lower than the energies of the stack configurations. To obtain a better description of the van der Waals interaction, the DFT results were corrected by adding a phenomenological van der Waals-type term into the total energy of the system. The problem with this approach is that the van der Waals correction is somewhat arbitrary, and different investigators choose different parameters, even for the same systems (cf., e.g., Refs. [21] and [22]). Depending on magnitude of the van der Waals term, both the T-shaped and the stack configurations can be the global minimum configuration of the system. Even though drawing the definitive conclusion is impossible at the currently achievable level of theory, it is quite surprising on its own that the T-shaped configuration is energetically competitive for such a large system for which a graphite-like stacked structure was expected [21].

To our knowledge, the present work is the first comparative study of the possible configurations of the coronine dimer performed within the ab initio approach. In the only other ab initio calculation of a coronene dimer [21], only a graphite-like (parallel-displaced) stacked structure was considered. There were also studies of the coronene dimer, which used phenomenological approaches [22, 26, 27]. In the most recent study of this type [22], the dimers and clusters of PAH molecules were modeled within a rigid-body approximation with the use of explicit interatomic potentials (a sum of an electrostatic and a van der Waals term). None of these studies used the semiempirical parameters that would make the T-shaped form of the coronene dimer energetically preferable. Therefore, the current result may lead to a completely different set of geometries of coronene clusters, which is an important issue for experimental and astrophysical studies [16].

We propose a simple model useful for qualitative understanding of dimerization and clusterization of PAHs. The model represents a PAH molecule as a set of circular or deformed rings corresponding to the chains of carbon atoms surrounded by a chain of hydrogens. For example, the coronene molecule is represented as a set of four nested circular rings, with the outer ring corresponding to the hydrogens. The electron density in PAHs is shifted from the hydrogens toward the interior of the molecules. In a crude approximation, this charge distribution can be described as a polarized band (with a positively charged outer edge and a negatively charged inner edge) located along the perimeter of a molecule. This charge distribution can also be considered as a dipole distributed along the border of a molecule. Two PAH molecules interact electrostatically and via the van der Waals forces between the sets of the rings substituting the monomers.

The model provides a qualitative explanation why even for such a large PAH as coronene ($C_{24}H_{12}$) the T-shaped configuration is comparable in energy to the stack configuration. This happens due to the round shape of the coronene molecule, leading to an increased electrostatic repulsion in the stack configurations. For non-round molecules in the stack configurations, the electrostatic interaction can be made less repulsive by rotating or by parallel displacement of the molecules in the dimer, while for stacked round molecules the rotation or displacement is much less effective, and the T-shaped configuration can become competitive.
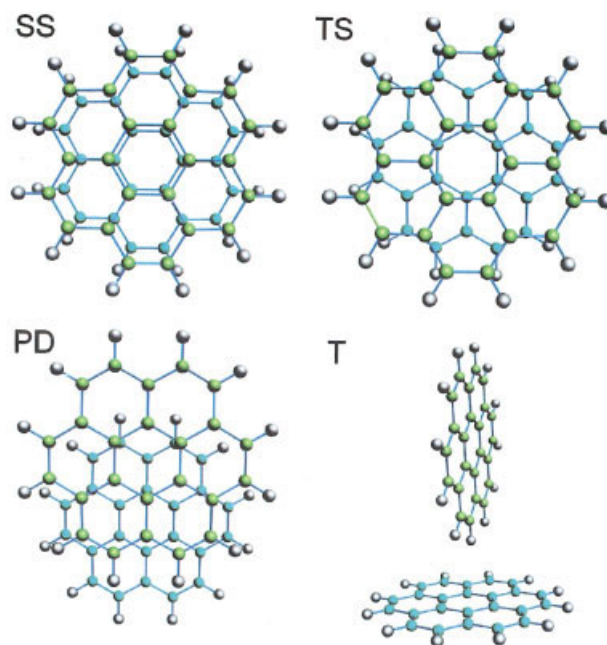

FIGURE 1. Geometries of four configurations of the coronene dimer optimized at the PBE/cc-pVTZ level of theory. In the sandwich (SS) configuration, the distance R between the centers of mass of the monomers equals 4.29 Å. In the twisted sandwich (TS) configuration, $R = 4.21$ Å, and the rotation angle is 30°. In the parallel-displaced (PD) configuration, $R = 3.95$ Å, and the shift is 2.70 Å. In the T-shaped (T) configuration $R = 8.02$ Å. The binding energies, calculated at various levels of theory, can be found in Table I. [Color figure can be viewed in the online issue, which is available at www.interscience.wiley.com.]

2. Dimer of Coronene

2.1. DENSITY FUNCTIONAL THEORY RESULTS

We have performed DFT calculations of binding energies for four configurations of coronene dimer. The dimer binding energy is defined as follows:

$$E_{b} = 2E_{mono} - E_{dimer}, \qquad (1)$$

where E_{dimer} is the total energy of the dimer and E_{mono} is the energy of the single molecule. According to this definition, the binding energies of the stable bound states of the dimer are positive.

The optimized studied geometries are shown in Figure 1, and the binding energies (counterpoise corrected) are summarized in Table I. The calcula-

	SS	TS	PD	T
B3LYP/6-31+G(d)[a]	−12.55	−9.16	−9.41	0.79
B3LYP/D95	−4.25	−4.15	−1.57	0.0034
B3LYP/cc-pVDZ	−5.18	−3.93	−4.02	0.0039
PBE/6-31+G(d)	−1.21	−0.87	0.061	0.88
PBE/D95	−4.24	−1.50	−0.11	1.12
PBE/cc-pVDZ	−1.98	−1.74	−0.91	0.84
PBE/cc-pVTZ	−0.99	−0.31	0.13	0.79
PBE/TZV(2d,2p), Ref. [21]	—	—	−4.89	—
BLYP/TZV(2d,2p), Ref. [21]	—	—	−17.52	—

* For notations and geometries of the dimer configurations, see Figure 1.
[a] Non-counterpoise corrected values.

tions have been done with the B3LYP and PBE functionals by expanding the molecular orbitals into the standard 6-31+G(d), D95, cc-pVDZ, and cc-pVTZ basis sets as implemented in the Gaussian 03 package [28, 29].

Calculations of geometries of the PAH oligomers present a difficult task because of the following two circumstances. First, the binding energies are rather small, sometimes smaller than the accuracy of the calculations. Second, the potential energy surfaces (PES) are very flat, leading to difficulties in finding the stable configurations. For the smallest aromatic hydrocarbon, benzene, the T-shaped configuration is almost isoenergetic (within accuracy margins of the calculations) with the parallel-displaced stack configuration [18–20]. In contrast, it is commonly believed that an increased number of aromatic rings favors stack configurations over the T-shaped ones [22, 24, 30]. In accord with this assumption, the T-shaped (or, more generally, "edge-to-plane") dimers of pyridine, naphthalene, azulene, and anthracene have been found less binding than the stacked configurations [15, 24, 25, 31]. Therefore, the larger the PAH molecule, the more reliable the predictions that can be made regarding the structures of its oligomers.

The present DFT results suggest that the dimer of coronene may be an exception from this general rule. The energy of the T-shaped configuration at all considered levels of theory was systematically lower than the energies of the three stack configu-

rations, quite a surprising result for such a large PAH molecule.

The reason for this unexpected behavior lies in the geometry of the coronene molecule leading to increased role of the electrostatic interaction, as discussed in Section 3. In addition to this physical argument, the obtained results can be justified by comparing the binding energies and geometries for an object for which reference data exist. The benzene dimer is the obvious choice. Such a comparison is done in Table II. It can be seen from Table II that the results of the PBE/cc-pVTZ method are in reasonably good agreement with the results of the more advanced calculations. Even better agreement is achieved by adding the phenomenological van der Waals terms as described in Section 2.2.

We note that the superimposed stack (sandwich) configuration probably is not a minimum on the PES. An analysis [22] done with the use of a phenomenological potential has identified it as a transitional state between the twisted stack and the parallel-displaced stack configurations. This conclusion is indirectly supported by the results of the high-level ab initio calculations that demonstrated that in benzene the superimposed stack is also a saddle point, rather than a true minimum [18].

2.2. PHENOMENOLOGICAL DFT+vdW AND MOLECULAR MECHANICS APPROACHES

One of the weaknesses of the pure DFT methods is that, at large distances, they do not reproduce the attractive polarization interactions well enough, for a discussion (see, e.g., Ref. [21] and references therein). This may present a serious problem in such intricate cases as determining the binding energy for loosely bound dimers of PAH molecules. To estimate the influence of the polarization van

	T
PBE/cc-pVTZ	0.74
PBE/cc-pVTZ + vdW[a]	1.82
CCSD(T)/aug-cc-pVDZ, Ref. [18]	2.17
CCSD(T)/CBS, estimate, Ref. [20]	2.39

[a] DFT + vdW method as described in Section 2.2 with parameters from Ref. [21].

TABLE III

Binding energies (in kcal/mol) for four configurations of the coronene dimer (see Figure 1) calculated according to expressions (1) and (2) for several sets of the coefficients C_6 (in J/mol nm^6) and C_{12} (in mJ/mol nm^{12}).*

	SS	TS	PD	T
$C_6^C = 2.77$ $C_6^H = 0.14$ $C_6^{C-H} = 0.63^a$				
$C_{12}^C = 4.87$ $C_{12}^H = 0.09$ $C_{12}^{C-H} = 0.68$	14.94 (15.93)	16.93 (17.24)	17.34 (17.21)	5.52 (4.73)
$C_6^C = 1.15$ $C_6^H = 0.11^{b\,c}$	6.62 (7.61)	8.10 (8.41)	8.64 (8.51)	3.09 (2.30)
$C_6^C = 0.88$ $C_6^H = 0.11^d$ $C_{12}^C = 4.87$ C_{12}^H				
$= 0.09^e$	2.34 (3.16)	4.01 (4.32)	4.32 (4.19)	1.88 (1.09)
Molecular mechanics	—	—	11.28	4.41
Pure PBE/cc-pVTZ ($C_6 = 0, C_{12} = 0$)	−0.99 (0.00)	−0.31 (0.00)	0.13 (0.00)	0.79 (0.00)

* Energies of the van der Waals terms are given in parentheses. The optimization of the dimer geometries and calculations of the DFT binding energies have been done with the PBE/cc-pVTZ method. The results of molecular mechanics simulations are given.
[a] From Ref. [32].
[b] From Ref. [21] (C_6 is adjusted by the factor 0.7 from one of the values (1.65) given in Ref. [33]).
[c] A dump function has been used instead of C_{12} [21].
[d] Another possible value (1.26) of the coefficient C_6^C from Ref. [33] multiplied by 0.7 as in Ref. [21].
[e] Coefficients C_{12} are from Ref. [32].

der Waals interaction on the preferred dimer geometry, we have included a phenomenological van der Waals-type term C_6/r^6 into the total energy of the system, similar to the procedure employed in Ref. [21]. To avoid too large a contribution from this term at smaller distances, C_6/r^6 is usually multiplied by a damping function vanishing exponentially at zero [21], or a repulsive C_{12}/r^{12} term is added:

$$E = E_{DFT} + \sum_{i,j} \left(\frac{C_{12}^{ij}}{r_{ij}^{12}} - \frac{C_6^{ij}}{r_{ij}^6} \right), \tag{2}$$

where E_{DFT} is the total energy of the system calculated within the frame of the DFT. Index i enumerates atoms in one monomer, and index j enumerates atoms in the other monomer; correspondingly, r_{ij} is the distance between atom "i" in the first monomer and atom "j" in the second monomer. The coefficients C_6^{ij} and C_{12}^{ij} can be tabulated directly (as in Ref. [32]) or found with the help of a combining rule (as is in Ref. [21]):

$$C_M^{ij} = 2 \frac{C_M^i C_M^j}{C_M^i + C_M^j}, \qquad M = 6, 12. \tag{3}$$

Unfortunately, there are no fixed values for coefficients C_6 and C_{12}, which would be universally applicable in a wide scope of situations. Even for the same systems, different investigators choose differ-

ent parameters (cf., e.g., Refs. [21] and [22]). The arbitrariness of the van der Waals correction appears to be a general problem of all such hybrid approaches.

To illustrate how sensitive the overall conclusions may be with respect to the values of the phenomenological parameters, Table III presents the binding energies for each of the considered dimer configurations for various choices of the parameters C_6^C, C_6^H, C_{12}^C, and C_{12}^H used in the literature. Depending on magnitude of the van der Waals term, both the T-shaped and the stack configurations can be the global minimum configuration of the system. The distance between the centers of mass of the monomers also varies very significantly depending on the choice of the parameters, from 3.55 Å to 4.3 Å in stack configurations. Table III also includes the results of the molecular mechanics calculations for the parallel-displaced and the T-shaped geometries. The parameters of the force field (CHARMM) were adjusted in such a way that the geometries and the binding energies of the benzene dimer are accurately reproduced.

Thus, we suppose that neither pure DFT, nor the hybrid DFT + van der Waals (DFT + vdW) or the molecular mechanics approaches, allows one to draw a definitive conclusion regarding the preferred geometry of the coronene dimer. We believe that an experimental measurement of the characteristics (e.g., frequencies of transitions between rota-

Rotational constants (in GHz) for different configurations of the coronene dimer calculated for the geometries optimized at B3LYP/D95 and PBE/D95 levels of theory.*

	SS			TS			PD			T	
B3LYP/D95	0.085	0.085	0.082	0.087	0.087	0.082	0.123	0.060	0.048	0.110	0.041	0.036
PBE/D95	0.087	0.087	0.082	0.089	0.089	0.082	0.113	0.074	0.059	0.111	0.041	0.037

* For notations and geometries of the dimer configurations, see Figure 1.

tional levels) would be useful for determining the global energy minimum configuration of the coronene dimer. To facilitate identification of the dimer configurations, Table IV presents the rotational constants for each configuration. The rotational constants B_η, connected to the principal values of the inertia tensor I as $B_\eta = \hbar/(4\pi I_{\eta\eta})$ ($\eta = x, y, z$), define the rotational levels $E_\eta = B_\eta J(J + 1)$ corresponding to different rotational quantum numbers J.

3. Rings Model of Polycyclic Aromatic Hydrocarbons

The model approaches not only can provide the estimates of the parameters of the systems, but sometimes they can also be very useful in revealing the underlying physics of a process and in pointing to the directions of search. We present a model that elucidates the role of the shapes of PAH molecules in the process of dimerization and in formation of bigger PAH clusters.

The model represents PAH molecules as a set of circular or deformed rings that correspond to the chains of carbon atoms surrounded by a chain of hydrogens. For example, the coronene molecule can be described as consisting of four concentric circular rings representing three chains of carbon atoms and one chain of hydrogens (see Fig. 2).

The electron density in PAHs is shifted from the hydrogens toward the interior of the molecules. Therefore, the outer ring (corresponding to the hydrogens) is always charged positively. The inner rings can, in principle, bear any charge, but their net charge, in the case of a neutral molecule, must be negative and must compensate the positive charge of the outermost ring.

The magnitude of charge for each ring is determined, for example, on the basis of the results of the DFT calculations as the sum of the partial charges of the atoms belonging to the corresponding ring.

Various methods can be used for assigning the partial charges to the atoms. For example, Mulliken suggested to calculate partial charges as the integral over the electron density contained within a sphere of a given radius, specific to the corresponding type of atoms [34]. Alternatively, one can expand the electron density into a set of natural bond orbitals (NBO) chosen in such a way that each orbital is occupied, ideally, by two electrons [35–37]. We use
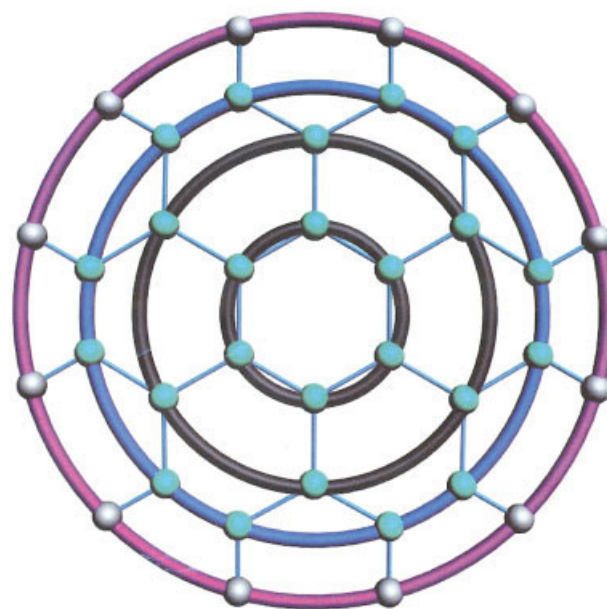

FIGURE 2. Round-shaped coronene molecule represented as a set of four nested circular rings. The radii of the rings are 1.438, 2.876, 3.595, and 4.691 Å ($R_{C—C}$ = 1.438 Å, $R_{C—H}$ = 1.096 Å). The outermost ring corresponds to the hydrogens and is positively charged. In the simplest case, this charge is compensated by the negative charge of the next ring, corresponding to the chain of outer carbon atoms. Two inner rings, then, are neutral. [Color figure can be viewed in the online issue, which is available at www. interscience.wiley.com.]

TABLE V

Partial charges in coronene assigned to carbon and hydrogen atoms according to the best fit electrostatic potential (ESP) [29] scheme (in units of elementary charge).*

	C_1	C_2	C_3	H
B3LYP/6-31+G(d)	−0.002	0.129	−0.207	0.148
B3LYP/D95	0.002	0.13	−0.237	0.168
B3LYP/cc-pVDZ	−0.004	0.095	−0.171	0.129
PBE/6-31+G(d)	−0.003	0.121	−0.223	0.148
PBE/D95	−0.003	0.133	−0.236	0.16
PBE/cc-pVDZ	−0.0002	0.086	−0.18	0.13
PBE/cc-pVTZ	0.002	0.114	−0.205	0.149

* C_1 are carbons from the innermost chain (there are 6 of them), C_2 are carbons from the intermediate carbon chain (6), C_3 are carbons from the outer carbon chain (12).

the so-called electrostatic potential scheme (ESP), in which the partial charges are determined from the best fit of the actual electrostatic potential of the molecule [29]. This method is not only better justified physically for our purposes, but it is also less dependent on the choice of the basis set used in the calculations, see Table V for the partial charges obtained.

In the simplest approximation, the electron density, shifted from the hydrogens, is assigned to the outer carbons, covalently bonded to the hydrogens. The ring corresponding to the chain of the outermost carbons is then charged negatively. The inner rings remain neutral. The charge distribution in such approximation can be crudely described as a polarized band (with a positively charged outer edge and a negatively charged inner edge) located along the perimeter of the molecule. This charge distribution can also be considered as a dipole continuously distributed along the outer border of the molecule. In fact, within this approximation, one can assign a typical value of the partial charge (say, 0.15 [32]) to all the hydrogen atoms, and one then immediately obtains the charges of the two outer rings. The DFT analysis of the electron density in this case is not necessary. This approximation provides a tool for studying interactions of large PAHs that cannot be treated with ab initio methods.

The interaction energy between two PAH molecules consists of a Coulomb and a van der Waals terms calculated for each pair of the rings:

$$E = \sum_{\alpha,\beta} (E_{\alpha\beta}^{\text{Coul}} + E_{\alpha\beta}^{\text{vdW}}), \qquad (4)$$

where index α enumerates the rings in one monomer, and index β enumerates the rings in the other monomer.

The energy of Coulomb interaction of two charged rings $E_{\alpha\beta}^{\text{Coul}}$ can be found by integrating the electrostatic potential created by one ring along the contour of the other ring:

$$E_{\alpha\beta}^{\text{Coul}} = \frac{Q_\beta}{|\ell_\beta|} \oint \phi_\alpha^{\text{Coul}}(\mathbf{r})\mathrm{d}\ell_\beta, \qquad (5)$$

where Q_β is the charge of the ring β equal to the sum of partial charges of all atoms belonging to the ring, $|\ell_\beta|$ is the length of the ring. The electrostatic potential $\phi_\alpha^{\text{Coul}}(\mathbf{r})$ created by a circular ring is expresses via the complete elliptic function K,

$$\phi_\alpha^{\text{Coul}}(\mathbf{r}) = \frac{2Q_\alpha}{\pi} \frac{1}{\sqrt{2rR_\alpha}} \frac{1}{\sqrt{x+1}} K\left(\frac{2}{x+1}\right), \qquad (6)$$

$$x = \frac{r^2 + R_\alpha^2}{2rR_\alpha \sin\theta}, \qquad (7)$$

where R_α is the radius of the ring α, r is the modulus of $\mathbf{r}$, and θ is the angle between $\mathbf{r}$ and the ring normal.

The van der Waals term $E_{\alpha\beta}^{\text{vdW}}$ can be calculated similarly:

$$E_{\alpha\beta}^{\text{vdW}} = \oint \left[\frac{Q_\beta^{\text{W}}}{|\ell_\beta|} \phi_\alpha^{\text{W}}(\mathbf{r}) + \frac{Q_\beta^{\text{X}}}{|\ell_\beta|} \phi_\alpha^{\text{X}}(\mathbf{r}) \right]\mathrm{d}\ell_\beta. \qquad (8)$$

The van der Waals charges Q^{W} and Q^{X} are defined as sums of the C_6 and C_{12} coefficients, respectively, of all the atoms belonging to the ring. For a circular ring, the van der Waals potentials ϕ^{W} and ϕ^{X} are expressed via elementary functions:

$$\phi_\alpha^{\text{W}}(\mathbf{r}) = \frac{Q_\alpha^{\text{W}}}{2} \frac{1}{(2rR_\alpha)^3} \frac{2x^2+1}{(x^2-1)^{5/2}}, \qquad (9)$$

$$\phi_\alpha^{\text{X}}(\mathbf{r}) = \frac{Q_\alpha^{\text{X}}}{8} \frac{1}{(2rR_\alpha)^6} \frac{x(8x^4 + 40x^2 + 15)}{(x^2-1)^{11/2}}. \qquad (10)$$

The model predicts the T-shaped and PD configurations to be stable in accordance with the results of the DFT calculations. The binding energies can be estimated to be 1.8 kcal/mol and 2.3 kcal/mol, respectively (for the magnitude of partial charges at the outer carbons and hydrogens of 0.1 and for van

der Waals parameters from Ref. [32]). This appears to be a reasonable estimate, even though the parameters of the model have to be carefully calibrated against reliable reference data before the model can be used to obtain quantitative results.

Importantly, the model provides an intuitively clear explanation for why even such a large PAH as coronene has a T-shaped configuration comparable in energy to that of the stack configuration. This happens because of the round shape of the coronene molecule, since only the "edge-to-plane" configurations can be stable electrostatically. In contrast, the dispersive interaction favors superimposed stacks for which the "contact area" is largest. For the non-round molecules (e.g., anthracene), the interplay between these two factors results in parallel-displaced or rotated configurations [24], because a parallel displacement or a rotation can significantly decrease the electrostatic repulsion while not seriously affecting the van der Waals attraction. However, for the round molecules, such as coronene, the rotation or parallel displacement is much less effective in decreasing the Coulomb repulsion, and the T-shaped configuration can become competitive.

We conclude that in the dimerization process (and in the formation of larger clusters of PAH molecules), the shapes of the molecules are very important. The proposed simple model can be useful in qualitative analysis of the possible configurations and in making the results of such analysis intuitively clear. The model can be applied to any PAH, and it can be easily generalized on the DNA bases, etc. The model can also be used for predicting structures of larger coronene clusters and clusters of other PAHs.

References

1. Langhoff, S. R. J Phys Chem 1996, 100, 2819.
2. Duley, W. W.; Lazarev, S. Astrophys J 2004, 612, L33.
3. Bernshtein, M. P.; Moore, M. H.; Elsila, J. E.; Sandford, S. A.; Allamandola, L. J.; Zare, R. N. Astrophys J 2003, 582, L25.
4. Allamandola, L. J.; Barker, J. P. Astrophys J 1985, 290, L25.
5. Bauschlicher, C. W.; Hudgins, D. M.; Allamandola, L. J. Theor Chem Acc 1999, 103, 154.
6. Duley, W. W.; Lazarev, S. Astrophys J 1981, 612, L33.
7. Leger, A.; Puget, J. L. Astron Astrophys 1984, 137, L5.
8. Sellgren, K. Astrophys J 1984, 277, 623.
9. Mattioda, A. L.; Allamandola, L. J.; Hudgins, D. M. Astrophys J 2005, 629, 1183.
10. Rapicioli, M.; Joblin, C.; Boissel, P. Astron Astrophys 2005, 429, 193.
11. Li, A. ASP Conf Ser 2004, 309, 417.
12. Puget, J. L.; Leger, A. An Rev Astr Ap 1989, 27, 161, and references therein.
13. Boulanger, F.; Abergel, A.; Bernard, J. P.; Cesarsky, D.; Puget, J. L.; Reach, W. T.; Ryter, C. ASP Conf Ser 1998, 132, 15.
14. Mitsui, M.; Kokubo, Sh.; Ando, N.; Matsumoto, Y.; Nakajima, A.; Kaya, K. J Chem Phys 2004, 16, 121.
15. Piuzzi, F.; Dimicoli, I.; Mons, M.; Millie, P.; Brenner, V.; Zhao, Q.; Soep, B.; Tramer, A. Chem Phys 2002, 275, 123.
16. Brechignac, Ph.; Schmidt, M.; Masson, A.; Pino, T.; Parneix, P.; Brechignac, C. Astron Astrophys 2005, 442, 239.
17. Duncan, M. A.; Khight, A. M.; Negishi, Y.; Nagao, S.; Kato, A.; Nakajima, A.; Kaya, K. Chem Phys Lett 1999, 309, 49.
18. Hobza, P.; Selzle, H. L.; Schlag, E. W. J Phys Chem 1996, 100, 18790.
19. Jaffe, R. L.; Smith, G. D. J Chem Phys 1996, 105(7), 2780.
20. Sinnokrot, M. O.; Valeev, E. F.; Sherrill, C. D. J Am Chem Soc 2002, 124, 10887.
21. Grimme, S. J Comput Chem 2004, 25, 1463.
22. Rapacioli, M.; Calvo, F.; Spiegelman, F.; Joblin, C.; Wales, D. J. J Phys Chem A 2005, 109, 2487.
23. Zhikol, O. A.; Shishkin, O. V.; Lyssenko, K. A.; Leszczynski, J. J Chem Phys 2005, 122, 144104.
24. Gonzalez, C.; Lim, E. C. J Phys Chem 2003, 107, 10105.
25. Grimme, S.; Piacenza, M. Chem Phys Chem 2005, 6, 1554.
26. Marzec, A. Carbon 2000, 38, 1863.
27. Miller, J. H.; Mallard, W. G.; Smyth, K. C. J Phys Chem 1984, 88, 4963.
28. Frisch, M. J.; Trucks, G. W.; Schlegel, H. B.; Scuseria, G. E.; Robb, M. A.; Cheeseman, J. R.; Montgomery, J. A., Jr.; Vreven, T.; Kudin, K. N.; Burant, J. C.; Millam, J. M.; Iyengar, S. S.; Tomasi, J.; Barone, V.; Mennucci, B.; Cossi, M.; Scalmani, G.; Rega, N.; Petersson, G. A.; Nakatsuji, H.; Hada, M.; Ehara, M.; Toyota, K.; Fukuda, R.; Hasegawa, J.; Ishida, M.; Nakajima, T.; Honda, Y.; Kitao, O.; Nakai, H.; Klene, M.; Li, X.; Knox, J. E.; Hratchian, H. P.; Cross, J. B.; Adamo, C.; Jaramillo, J.; Gomperts, R.; Stratmann, R. E.; Yazyev, O.; Austin, A. J.; Cammi, R.; Pomelli, C.; Ochterski, J. W.; Ayala, P. Y.; Morokuma, K.; Voth, G. A.; Salvador, P.; Dannenberg,

J. J.; Zakrzewski, V. G.; Dapprich, S.; Daniels, A. D.; Strain, M. C.; Farkas, O.; Malick, D. K.; Rabuck, A. D.; Raghava-chari, K.; Foresman, J. B.; Oritz, J. V.; Cui, Q.; Baboul, A. G.; Clifford, S.; Cioslowski, J.; Stefanov, B. B.; Liu, G.; Liashenko, A.; Piskorz, P.; Komaromi, I.; Martin, R. L.; Fox, D. J.; Keith, T.; Al-Laham, M. A.; Peng, C. Y.; Nanayakkara, A.; Challa-combe, M.; Gill, P. M. W.; Johnson, B.; Chen, W.; Wong, M. W.; Gonzalez, C.; Pople, J. A. Gaussian 03; Revision C.02; Gaussian: Wallingford, CT, 2004.

29. Foresman, J. B.; Frisch, A. Exploring Chemistry with Elec-tronic Structure Methods; Gaussian: Pittsburgh, PA, 1996.

30. Jorgensen, W. L.; Severance, D. L. J Am Chem Soc 1990, 112, 4768.

31. Piacenza, M.; Grimme, S. J Am Chem Soc 2005, 127, 14841.

32. van de Waal, B. W. J Chem Phys 1983, 79, 3948.

33. Wu, Q.; Yang, W. J Chem Phys 2002, 116, 515.

34. Mulliken, R. S. J Chem Phys 1955, 23, 1833.

35. Lowdin, P. O. Phys Rev 1955, 97, 1474.

36. Carpenter, J. E.; Weinhold, F. Theor Chem Acc 1988, 169, 141.

37. Weinhold, F.; Landis, C. R. Chem Ed Res Pract Eur 2001, 2, 91.